

Sculpting priors

James Theiler

Space Remote Sensing and Data Science Group,
Los Alamos National Laboratory,
Los Alamos, NM 87545, USA

ABSTRACT

Bayesian priors are investigated for detecting targets of known spectral signature (but unknown strength) in cluttered backgrounds. A specific problem is the construction (or “sculpting”) of a Bayesian prior that uniformly outperforms its non-Bayesian counterpart, the nominally sub-optimal but widely used Generalized Likelihood Ratio Test (GLRT).

1. INTRODUCTION

This study is motivated by the problem of detecting targets in cluttered backgrounds. The specific example considered here is the detection of solid sub-pixel targets in multispectral (or hyperspectral) imagery [1–9]. Although there are many variants and real-world complications, a simple statement of the problem considers a target with spectral signature \mathbf{t} and abundance (*i.e.*, size relative to a pixel) a , against a background \mathbf{z} , leading to a measured pixel value

$$\mathbf{x} = (1 - a)\mathbf{z} + a\mathbf{t} \quad (1)$$

Here, \mathbf{t} , \mathbf{z} , and \mathbf{x} are d -dimensional vectors (elements of \mathbb{R}^d), corresponding to the d spectral channels of the imaging sensor; and a is a scalar bounded between 0 and 1.

In this expression, \mathbf{t} is known (it is typically measured in the laboratory, or directly from the sensor at locations where the target is known to cover a full pixel), and although the background \mathbf{z} is not known in detail, it is assumed to be drawn from a distribution $P_{\text{bkg}}(\mathbf{z})$ that is known (it is usually inferred from measurements over a large number of presumably [or at least mostly] target-free pixels). In terms of the target abundance a , we can write the distribution associated with the measured pixel:

$$P_{\text{tgt}}(a, \mathbf{x}) = (1 - a)^{-d} P_{\text{bkg}}\left(\frac{\mathbf{x} - a\mathbf{t}}{1 - a}\right). \quad (2)$$

Note that $P_{\text{tgt}}(0, \mathbf{x}) = P_{\text{bkg}}(\mathbf{x})$.

The basic goal, here, is to find targets – in the case of imagery, to identify the pixels in which the targets appear. Specifically, we seek a function $\mathcal{D}(\mathbf{x})$ that maps the observed vector \mathbf{x} to a scalar that correlates with target presence. Targets are identified by comparing $\mathcal{D}(\mathbf{x})$ to a threshold η . Values of $\mathcal{D}(\mathbf{x})$ above the threshold correspond to targets, and values below the threshold are taken to be target-free. A bit of terminology: the real-valued function $\mathcal{D}(\mathbf{x})$ is called a “detection statistic” while the binary function given by comparing $\mathcal{D}(\mathbf{x})$ to a threshold η is called a “decision rule.” The term “detector” is used informally (and sometimes ambiguously) to refer to one or the other (or sometimes both).

There are (at least) two different approaches for obtaining a detection statistic $\mathcal{D}(\mathbf{x})$: estimation and hypothesis testing. An *estimator* is a function $\hat{a}(\mathbf{x})$ that aims to approximate the true abundance a . A typical (but not the only available) choice is the maximum likelihood estimator

$$\hat{a}(\mathbf{x}) = \operatorname{argmax}_a P_{\text{tgt}}(a, \mathbf{x}). \quad (3)$$

If we want to know if and/or where targets might be in a given image (or corpus of images) we could do worse than computing $\hat{a}(\mathbf{x})$ over all the pixels, and then taking as targets those pixels for which the value is above some threshold. But we could also do better.

The hypothesis testing approach aims to more directly infer whether a is zero or non-zero. For the *simple* hypothesis testing problem, there are only two alternatives: $a = 0$ and $a = a_o$ for some $a_o > 0$ that is specified beforehand. This is sometimes referred to the “clairvoyant” case [10]. It is a conceptually useful case, even as it is unrealistic in those cases for which the nonzero target strength a_o is *not* known *a priori*. What is useful about it is that it has an unambiguously optimal solution, given by the likelihood ratio:

$$\mathcal{D}_c(a_o, \mathbf{x}) = \frac{P_{\text{tgt}}(a_o, \mathbf{x})}{P_{\text{bkg}}(\mathbf{x})}. \quad (4)$$

1.1. Measures of detector quality

A good detector will find most of the targets with only a few false alarms. Thus we seek to maximize the detection rate (DR)

$$\text{DR} = \int_{\mathcal{D}(\mathbf{x}) \geq \eta} P_{\text{tgt}}(a, \mathbf{x}) \, d\mathbf{x} \quad (5)$$

while minimizing the false alarm rate (FAR)

$$\text{FAR} = \int_{\mathcal{D}(\mathbf{x}) \geq \eta} P_{\text{bkg}}(\mathbf{x}) \, d\mathbf{x}. \quad (6)$$

Note that both of these quantities depend on the threshold η . Decreasing η will generally increase the detection rate, but at the expense of also increasing the false alarm rate. A plot of DR vs FAR as η varies defines the so-called Receiver Operating Characteristic (ROC) curve. The *power* of a detector is its detection rate at the threshold η that corresponds to a given false alarm rate. The area-under-the-curve (AUC) statistic corresponds to the area under the ROC curve – it is a sort of average power, with the average taken over all false alarm rates from 0 to 1. Another criterion that is often of interest in detection problems is the false alarm rate at a fixed detection rate.

It is important to observe that DR depends on the target strength a . A consequence of this is that it is possible for one detector to be better (that is, to be more powerful) than another detector at one value of a , and worse than that other detector at some other value of a . A *uniformly* more powerful detector will be better at all values of a . (To be a little more precise: a uniformly more powerful detector will be as good or better at all values of a , and strictly better at at least one value of a .)

For a known fixed target strength $a = a_o$, the optimal detector is given by the likelihood ratio in Eq. (4).

In practice, however, a may not be a known fixed quantity. In fact, there are two senses in which a is not known: 1/ it is not known whether the target is present in the given pixel, so we do not know if a is zero or nonzero; and 2/ presuming a is nonzero, we do not know which nonzero value it has. Because our ignorance of a extends into this second case, our problem becomes one of *composite hypothesis testing*, and we cannot use the simple likelihood ratio in Eq. (4).

The non-Bayesian approach is to employ the likelihood ratio using the maximum-likelihood estimator for $a_o = \hat{a}(\mathbf{x})$. This leads to the Generalized Likelihood Ratio Test (GLRT):

$$\mathcal{D}(\mathbf{x}) = \frac{\max_a P_{\text{tgt}}(a, \mathbf{x})}{P_{\text{bkg}}(\mathbf{x})}. \quad (7)$$

The Bayesian approach is to identify a prior $q(a)$ and to average the likelihood with respect to that prior:

$$\mathcal{D}(\mathbf{x}) = \frac{\int P_{\text{tgt}}(a, \mathbf{x}) q(a) \, da}{P_{\text{bkg}}(\mathbf{x})}. \quad (8)$$

A classic result in the theory of hypothesis testing [11] is that Bayesian detectors (strictly speaking: decision rules) are *admissible*, and that all admissible detectors are either Bayesian or can be expressed as a limit of Bayesian detectors. A detector is admissible if no other detector is uniformly more powerful. It follows that for any given detector $\mathcal{D}(\mathbf{x})$ there must exist a prior function $q(a)$ such that the Bayesian detector associated with that prior (that is, the Bayesian detector defined in Eq. (8)) is uniformly as powerful or more powerful than $\mathcal{D}(\mathbf{x})$. This motivates our interest in constructing a prior that enables the Bayesian detector to equal or beat any non-Bayesian detector.

As a side note, there is a further class of detectors [12–15] that generalize the the GLRT by incorporating a function $q(a)$ that is superficially similar to the prior in Eq. (8). Here,

$$\mathcal{D}(\mathbf{x}) = \frac{\max_a P_{\text{tgt}}(a, \mathbf{x})q(a)}{P_{\text{bkg}}(\mathbf{x})}. \quad (9)$$

These are not Bayesian detectors (because the “max” is not the same as an integral), and therefore may not be admissible, but the $q(a)$ does provide a flexibility that is not available in the standard GLRT.

1.2. Interpreting the prior: detectors vs estimators

“It is a capital mistake to theorize before one has data. Insensibly, one begins to twist facts to suit theories, instead of theories to suit facts.”
 – Arthur Conan Doyle, *A Scandal in Bohemia*.

A popular interpretation of the Bayesian prior is that it represents an initial data-free guess (some would say: belief) for what values a parameter might take on. There is an inherent subjectiveness in this interpretation (perhaps the very kind of subjectiveness that Sherlock Holmes warns against), and a premium is placed upon priors that are broad, flat, and uninformative. In this view, the worst mistake of all is to employ a prior that is a delta-function about a single value.

But it is important to recognize that this interpretation of the prior is only appropriate for *estimation* problems. For example, if our aim is to estimate a , and our prior is $\delta(a - a_o)$, then the posterior estimate will always be $\hat{a} = a_o$, regardless of what data are observed. (Put another way: no matter what we observe, our conclusion will coincide with our initial prejudice.) On the face of it, it is not obvious that detection and estimation are all that different. Indeed, it is not a terrible idea (it is usually sub-optimal, but not terrible) to detect targets by estimating a candidate target’s strength, and then checking to see if that estimate is sufficiently nonzero.

But in fact, estimation is different from hypothesis testing. And for detection via hypothesis testing, the prior need not be a subjective guess, but instead can express objective criteria. Given a specific criterion to be optimized, one can turn around* and construct (or “sculpt”) the prior that optimizes this criterion. It also bears remarking that for the detection problem, a delta-function prior is not necessarily a bad idea (indeed, it is the basis of the *veritas* algorithm [16]).

2. SCULPTING PRIORS

The task we have set out for ourselves is to identify a prior function $q(a)$ with the property that it permits the associated Bayesian detector to uniformly outperform the GLRT detector. We have seen previously [17] that this is not always possible for some performance criteria (eg, FAR at fixed DR), but for other criteria (eg, DR at fixed FAR; or AUC), it is guaranteed to be possible by the theory [11].

In the full problem, a is allowed to vary continuously from 0 to 1. To enable numerical exploration of optimal priors, we will restrict the prior to be a “delta comb.” That is, for a fixed number K , the prior is given by K weights $\mathbf{w} = [w_1, \dots, w_K]$ and K values of a (called “knots”): $\mathbf{a} = [a_1, \dots, a_K]$.

$$q(a) = \sum_{k=1}^K w_k \delta(a - a_k). \quad (10)$$

*Indeed, the very term “turn around” implies (correctly) that this is a kind of inverse problem.

The use of delta-comb priors is a restriction, not an approximation. The Bayesian detectors that employ these priors are computed exactly (to within numerical precision), and the resulting decision rules are, in a strict and formal sense, admissible.

The *veritas* algorithm [16] is a special case in which $K = 1$ and the value of a_1 is carefully chosen. Here, we will consider larger values of K and let a_k uniformly fill the interval; in particular, we'll divide the unit interval into K equal segments and place the k th knot at the midpoint[†] of the k th segment: thus, $a_k = (k - 1/2)/K$.

In the evaluation of these delta-comb priors, we will consider only the values of a that are part of the delta-comb itself. That is, the problem itself has been modified so that the unknown target abundance a is assumed to be either zero (no target) or one of the delta-comb values in \mathbf{a} . Not only does this simplify the numerics, but it means that in the context of the problem, we are considering *all* possible Bayesian priors. Given this restriction, we will also consider a restricted version of the GLRT (that we'll call the RGLRT) that also only considers the abundances in \mathbf{a} . To be more specific:

$$\mathcal{D}_{\text{GLRT}}(\mathbf{x}) = \max_{a \in [0,1]} \frac{P_{\text{tgt}}(a, \mathbf{x})}{P_{\text{bkg}}(\mathbf{x})}, \quad (11)$$

$$\mathcal{D}_{\text{RGLRT}}(\mathbf{x}) = \max_{a \in \mathbf{a}} \frac{P_{\text{tgt}}(a, \mathbf{x})}{P_{\text{bkg}}(\mathbf{x})}. \quad (12)$$

For small values of K , we find that the RGLRT outperforms the GLRT. For larger values of K , the two detectors become more nearly equal and exhibit more nearly equal performance. A practical distinction between the two is that GLRT is typically evaluated by taking the derivative of the likelihood ratio and setting that derivative to zero, thus leading to a single closed-form expression. The RGLRT solution is also, technically speaking, a closed-form expression, but its evaluation requires the computation of K separate likelihood ratios; thus, especially for larger K , the RGLRT can be more computationally expensive.

Since we are specifically looking to find Bayesian weights that outperform the associated (R)GLRT detector, we will seek to optimize the loss function

$$\begin{aligned} \mathcal{L}(\mathbf{w}) &= \max_a L(a, \mathbf{w}), \text{ where} \\ L(a, \mathbf{w}) &= s_{\text{Bayes}}(\mathbf{w}, a) - s_{\text{RGLRT}}(a) \end{aligned} \quad (13)$$

where s is a ROC-based performance statistic (with smaller s being better), such as FAR@DR=0.5, or 1-DR@FAR=0.05 or 1-AUC. If we can find \mathbf{w} such that $\mathcal{L}(\mathbf{w}) \leq 0$, then that implies that $L(a, \mathbf{w}) \leq 0$ for every a , which implies that the Bayesian detector has uniformly matched or outperformed the GLRT-based detector.

3. EXPERIMENTS

We perform numerical experiments with a large sample of points drawn from simulated elliptically-contoured multivariate t -distributed data. This distribution can be expressed in closed-form

$$P_{\text{bkg}}(\mathbf{x}) = c [\nu - 2 + (\mathbf{x} - \boldsymbol{\mu})^T R^{-1}(\mathbf{x} - \boldsymbol{\mu})]^{-(\nu+d)/2} \quad (14)$$

where c is a normalizing constant, and ν is the “degrees of freedom” parameter – small ν corresponds to a fat tail, and $\nu \rightarrow \infty$ leads to a Gaussian distribution. Under this distribution, the GLRT can also be expressed in closed form [1, 5], as can the clairvoyant detector [16], and therefore any Bayesian detector with a finite delta-comb prior.

We use zero mean ($\boldsymbol{\mu} = 0$) and unit covariance ($R = I$). (This does not really cause any loss of generality, since our detection algorithm would be whitening the data anyway – we'll be using very large sample size, so the covariance would be accurately approximated.) We take $\nu = 3$, which indicates a very non-Gaussian fat-tailed distribution.

[†]We avoid $a = 0$ since that corresponds to no target, but in fact, we could consider a term corresponding to the $a \rightarrow 0$ limit, using an approach described in Ref. [18].

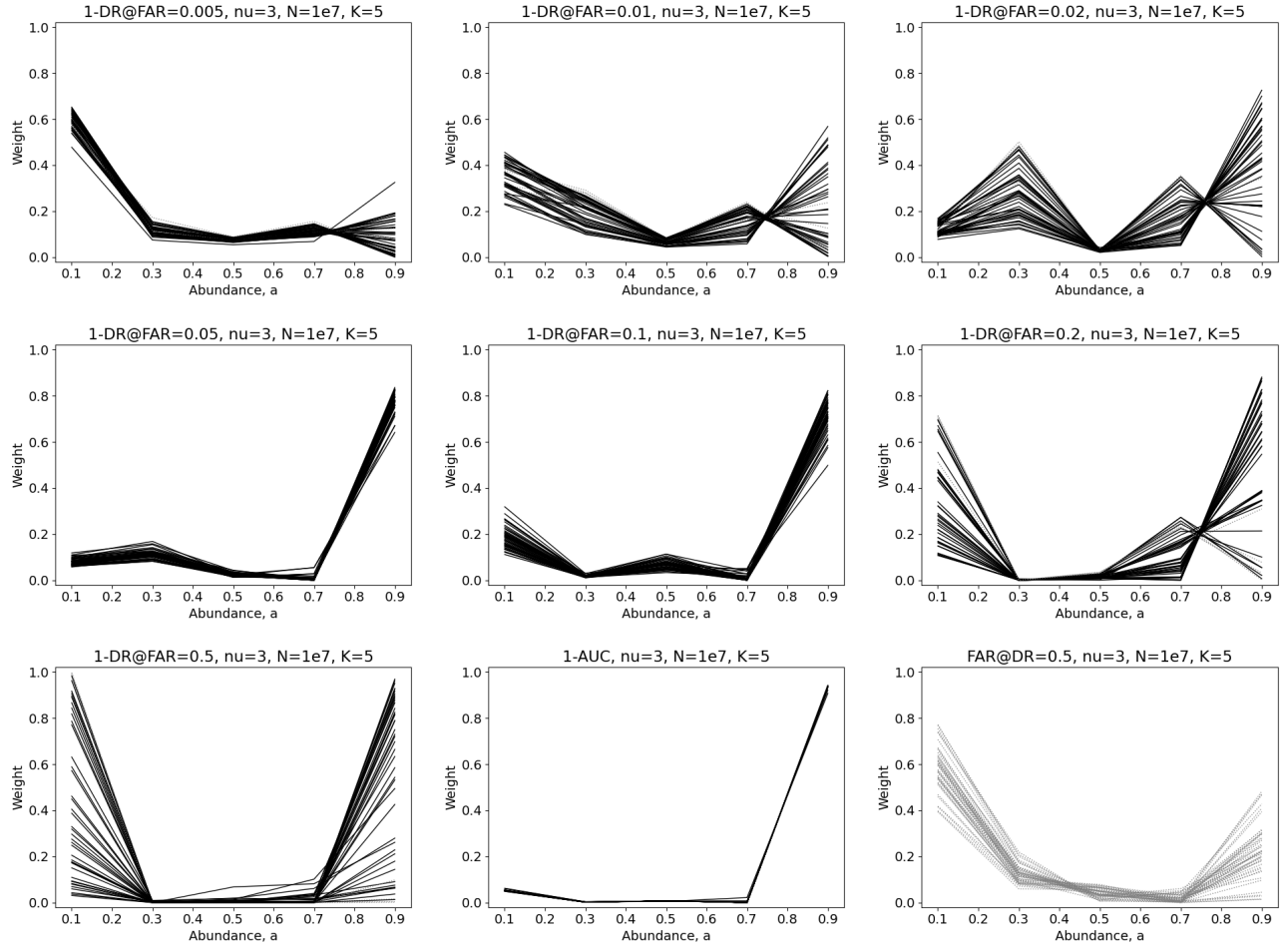


Figure 1. Plot of weights $[w_1, \dots, w_K]$ against abundance values $[a_1, \dots, a_K]$, with $K = 5$, for the delta-comb prior defined in Eq. (10). These weights optimize the loss function in Eq. (13), as computed with $N = 10^7$ samples, and based on different ROC-based statistics. The first seven panels are of for $\text{DR@FAR}=x$ for various (increasing) values of x . The last two panels show results for the AUC statistic and for $\text{FAR@DR}=0.5$. Results are shown from 45 trials, with solid lines indicating solutions with $\mathcal{L}(\mathbf{w}) \leq 0$ and dotted lines for solutions with $\mathcal{L}(\mathbf{w}) > 0$. Note that almost all of the lines are solid in these plots, *except* for the $\text{FAR@DR}=0.5$ statistic in the last panel. This is consistent with the theory that guarantees the existence of priors for which Bayesian detection is uniformly at least as powerful as any given detector, when evaluated with AUC or the DR-based statistics. The theory does not apply to the FAR-based statistics [17]; in this case there appears not to be any prior that leads to uniform superiority, but other cases have been found (see Fig. 7) in which the Bayesian detector is uniformly better.

In the first batch of experiments, $d = 9$ spectral channels, $N = 10^7$ target-free pixels, and $N = 10^7$ corresponding pixels for each nonzero target strength a in the delta-comb. Note that these are matched-pair pixels [19], with each target-present pixel matched to a specific target-absent pixel in which target has been added. As a way of assessing variability in the estimate of the prior weight vector \mathbf{w} (which will depend on the particular sample of N points), we run 45 trials, and each trial is plotted separately in the figures.

The qualitative goal of this study was to see what the priors look like that enable Bayesian detectors to outperform their non-Bayesian (GLRT) counterparts. What was found is that the shape of a high-performing prior depends on the particular choice of detection statistic that is being optimized. In Fig. 1, nine such statistics are considered, the first seven of which are of the form $\text{DR@FAR}=x$, for different values of x . Despite the similarity of these statistics, the shapes of those priors vary considerably for different values of x . The AUC

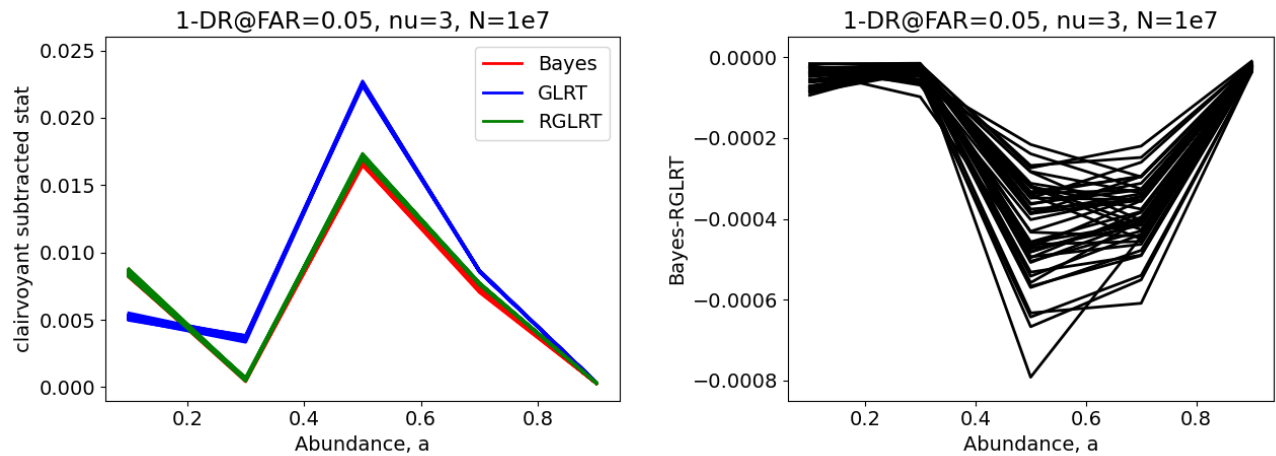


Figure 2. Performance differences: Left panel shows 1-DR@FAR=0.05 statistic for Bayes, GLRT, and RGLRT statistics, with the clairvoyant performance subtracted. We observe that these differences are all positive, which demonstrates the known result that the clairvoyant detector is optimal (though in practice it is usually unavailable). Right panel shows the difference of Bayesian and RGLRT detectors. Here all values are negative, which indicates that the Bayesian detector is uniformly more powerful than RGLRT. It bears remarking that the magnitude of these differences is small. These methods are all within a few percent of the clairvoyant detection rate, and the difference between Bayes and RGLRT is less than a tenth of a percent, often much less.

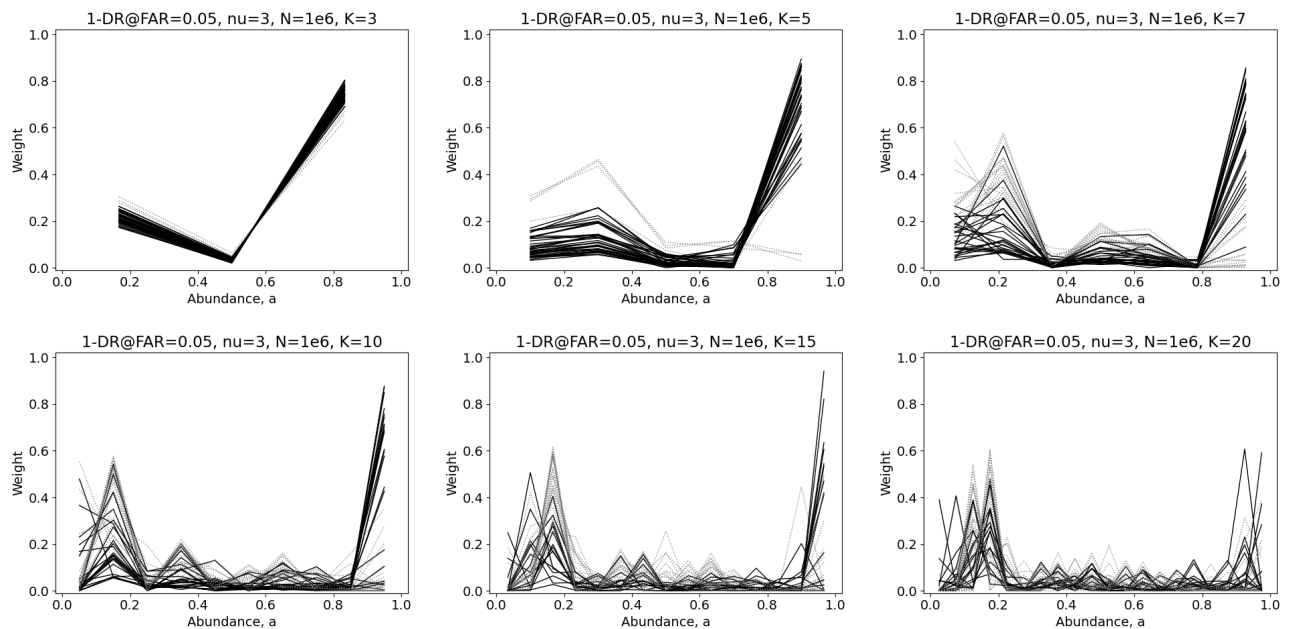


Figure 3. Priors that optimize the DR@FAR=0.05 statistic for increasing number of knots K .

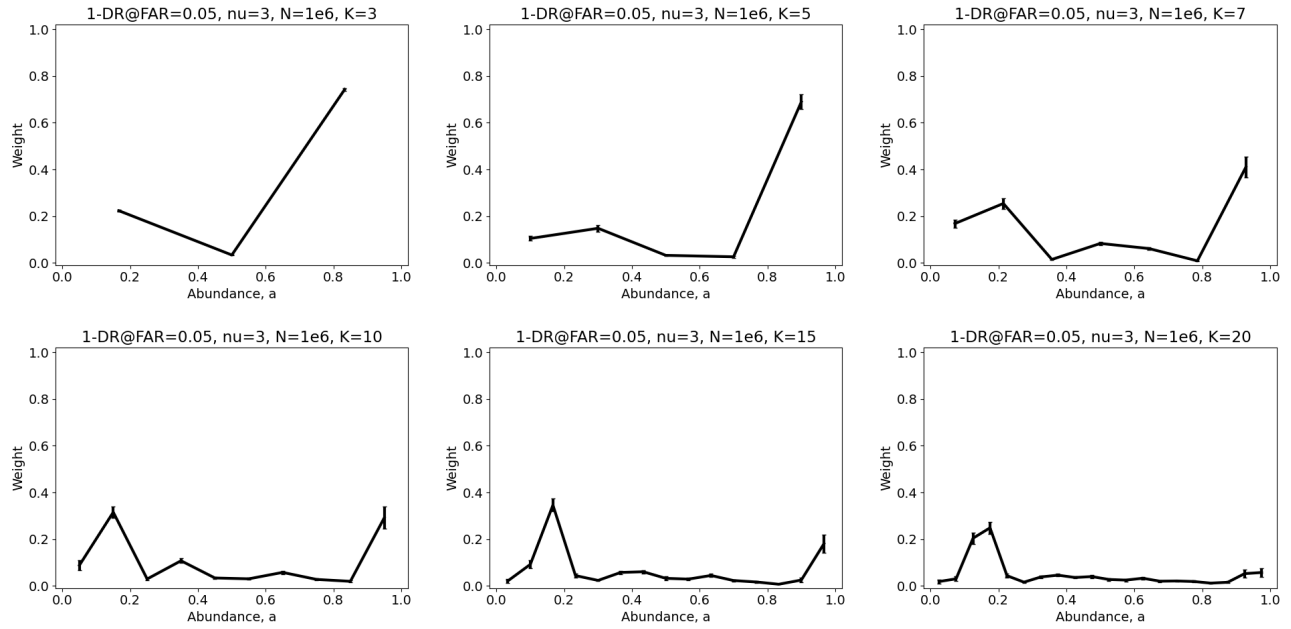


Figure 4. Priors that optimize the DR@FAR=0.05 statistic for increasing number of knots K . Shown is a mean of 45 trials, with error bars indicating standard error.

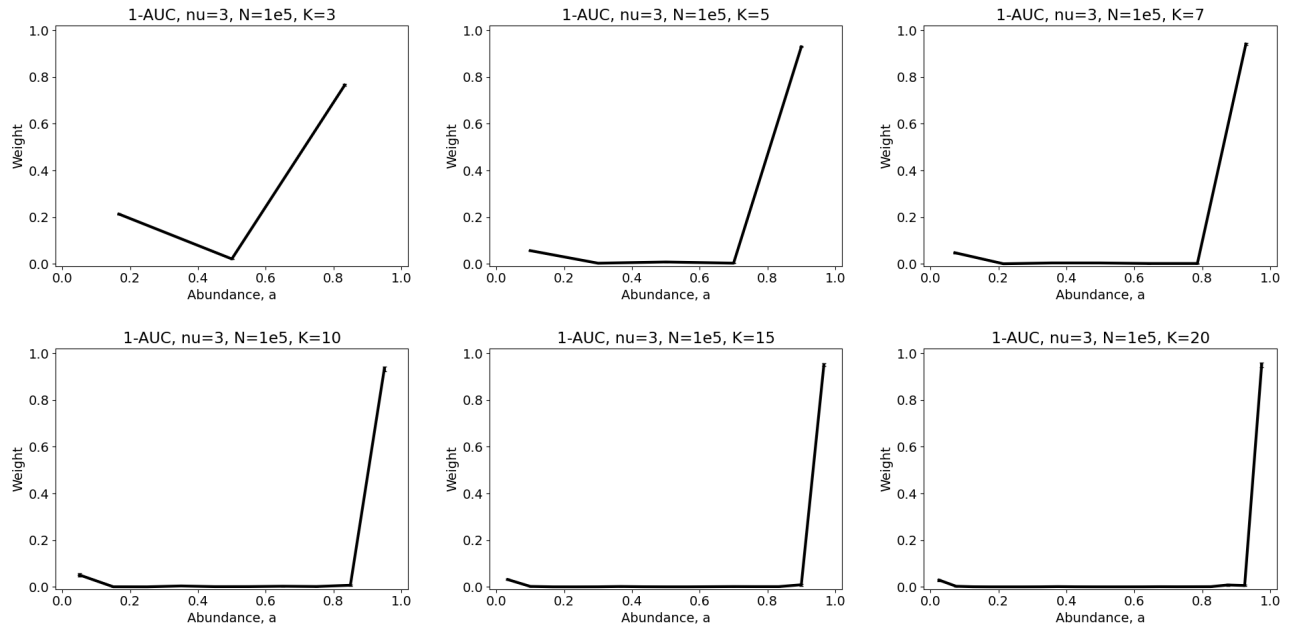


Figure 5. Priors that optimize the AUC statistic for increasing number of knots K . Shown is a mean of 45 trials, with error bars indicating standard error. These plots suggest that, from the point of view of optimizing AUC, a very good detector might be the simple likelihood ratio in the limit as $a \rightarrow 1$.

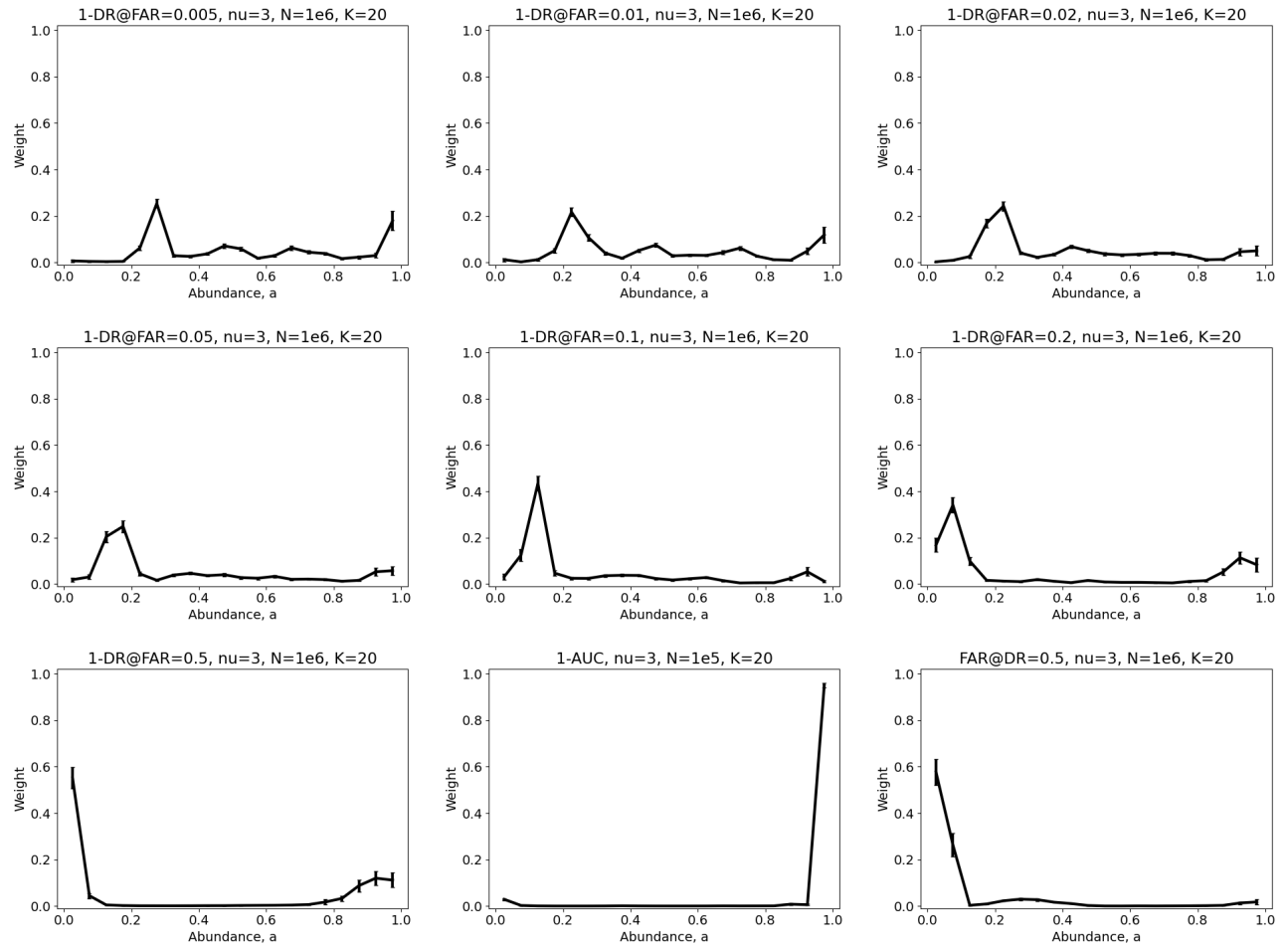


Figure 6. Prior weights for various performance criteria; using $K = 20$, and averaging over 45 trials.

statistic, seen in the eighth panel of Fig. 1, and the FAR@DR=0.5 statistic, seen in the ninth panel, exhibits yet other shapes. Also evident from these figures: not only do the shapes vary, but the amount of trial-to-trial variability in high-performing priors also varies considerably with choice of statistic.

Although we speak of Bayesian detectors (with appropriately sculpted priors) being uniformly more powerful than their GLRT counterparts, it is worth keeping in mind, at least for the experiments reported here, that the actual performance differences are quite small. Fig. 2 shows that these detectors exhibit detection rates that are only one to two percent higher than the optimal clairvoyant detectors, and that the differences between Bayes and RGLRT is less than a tenth of a percent.

In assessing the qualitative shape of successful priors, we would ultimately like to consider continuous functions $q(a)$, but for numerical reasons we stick to the discrete case with a bounded number K of knots. Fig. 3 shows what the optimal prior looks like for the DR@FAR=0.05 statistic, and we observe increasingly complicated curves for increasing K . The general trend for all these trials is to put most of the weight near $a = 0.18$ or so, with higher weights also near $a = 1$, but also some weight for a range of a between those values. To some extent, the jaggedness of these curves reflects the numerical challenges of optimization in a space of high dimension – that dimension is $K - 1$, arising from the K weights, minus the one constraint that weights sum to one. The trend is easier to see in Fig. 4, which is the average of the 45 trials.

A contrasting situation is seen in Fig. 5, which considers the same question for the AUC statistic. In this case, the curves appear to be approaching an almost singular function with almost all of the weight concentrated near $a = 1$. As noted in Ref. [16] (see Eq.(28) of that reference), we can express the detector associated with $a \rightarrow 1$ in closed form.

Finally, in Fig. 6, the mean sculpted priors for $K = 20$ are shown for the same nine ROC statistics that were used in Fig. 1.

4. CONCLUDING DISCUSSION

Admissibility is a good thing, but the fact that Bayesian decision rules are admissible doesn't mean Bayesian detectors are *always* better; this was shown previously [17] in the context of FAR@DR= x statistics. What is shown here is that even when Bayesian detectors *are* better (as is the case for DR@FAR= x and AUC statistics), this theoretical superiority comes with some practical disadvantages. What we've observed in the experiments shown here is that when Bayesian detectors are better than the non-Bayesian GLRT or RGLRT detectors, they are better by a tiny amount. Furthermore, in order to achieve these tiny advantages, the priors must be very carefully (and expensively) sculpted – and a prior that works (*i.e.*, that achieves an incrementally higher detection rate than the associated non-Bayesian detector) for one criterion will not work for a related criterion.

On the other hand, we can turn this argument around and point out that the difference between two Bayesian detectors, which differ in their choice of prior, is often fairly small, so that a detector that is built from a generic non-sculpted prior may still be useful. A particular example is the *veritas* detector, which is Bayesian with a single delta-function prior. One practical advantage of this detector is that the Bayesian integral is straightforward and can lead to simple closed-form expressions for the detector, even when the background model is relatively complicated.

A second advantage to Bayesian detectors is that they work well in a matched-pair machine learning scenario [19]. In this case, we do not have an explicit model for $P_{\text{bkg}}(\mathbf{x})$, but instead use discriminative machine learning to distinguish between $P_{\text{bkg}}(x)$ and $P_{\text{tgt}}(a, x)$. In this scenario, we have a population of target-free data (the original pixels in the image) and a corresponding population of pixels into which targets have been implanted. The sculpted prior provides a distribution for target strengths a to be used in generating the implanted target pixels.

5. ACKNOWLEDGMENTS

I am grateful: to the Laboratory Directed Research and Development (LDRD) program at Los Alamos National Laboratory for support; to Stefania Matteoli for valuable discussions about Bayesian detection; and to Tory Carr for asking the question, after seeing a talk I gave on Ref. [17], “Well, what *would* those priors look like?”

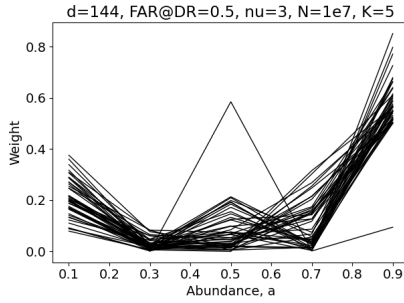


Figure 7. Example in which priors can be found that lead to uniformly more powerful Bayesian detectors using the FAR@DR=0.5 statistic. This is similar to the last panel in Fig. 1 except that $d = 144$ instead of $d = 9$. Here, all the curves are solid (Bayes wins), while in Fig. 1, the curves are dotted (indicating that Bayes is *not* uniformly better).

APPENDIX A. SOME TECHNICAL DETAILS

Because the performance differences (as seen in Fig. 2 for instance) are so small, it takes very large sample sizes N (upwards of ten million samples) in order to determine which detector achieved the best performance. Even with these large sample sizes, considerable variability was observed from one batch of samples to the next. In general, 45 batches were used for each experiment so that this variability could be assessed (and averaged over).

The numerical problem of finding weights w_1, \dots, w_K to optimize the given performance statistic was more difficult than originally expected. Evaluating the performance for a given set of weights is somewhat expensive, with $O(NK^2)$ steps required. (One factor of K arises from the K terms in the Bayesian sum, and the other factor from the need to evaluate that sum for each of the K knots.) Further, the evaluation only provides a scalar performance metric, so optimization schemes that require a gradient cannot be directly employed. In terms of the optimizers in the `scipy.optimize` tools[‡], this reduces to: Powell’s method, Nelder-Mead (sometimes called the “simplex” method), and COBYLA (Constrained Optimization BY Linear Approximation). For the sculpting priors problem, all three of these exhibited inconsistent convergence (particularly for larger values of K), though COBYLA was much faster, so some initial results were obtained by using many random initial guesses, applying COBYLA to each, and choosing the one with the smallest optimum value.

For the results shown here, however, a klunky home-grown optimizer (called “babysteps”) was employed. Although we do not have a gradient, *per se*, we do know that increasing the weight w_k at a given knot a_k will improve the performance of the Bayesian detector at that knot. The idea is to increase the weight associated with the knot that most needs it. This increase is by a small amount (a baby step), and all the weights are subsequently rescaled so the sum of weights is equal to one. This process of getting a new set of weights is then iterated. In this work a fixed step size and fixed number of iterations were used.

Using a specified ROC-based statistic, the RGLRT detector is evaluated for each target strength a_1, \dots, a_K . Since RGLRT does not depend on weights, this evaluation, which provides $s_{\text{RGLRT}}(a_k)$ for each a_k need only be done once.

For each iteration of the babysteps algorithm, we begin with a set of weights $\mathbf{w} = [w_1, \dots, w_K]$, and evaluate the Bayesian detector at each a_1, \dots, a_k . Since our loss function is of the form $L(\mathbf{w}) = \max_k L(\mathbf{w}, a_k)$ as seen in Eq. (13), it is clear that $k_* = \operatorname{argmax}_k L(\mathbf{w}, a_k)$ is the knot most in need of improvement. So we update the weights with $w_{k_*} \leftarrow w_{k_*} + \Delta w$ (where typically $\Delta w = 0.01$), followed by $w_k \leftarrow w_k / (1 + \Delta w)$ for all $k = 1, \dots, K$.

As was briefly mentioned in the caption to Fig. 1, with respect to the theory guaranteeing the existence of priors that lead to uniformly superior behavior for Bayesian detectors, that theory does not apply for the FAR@DR=0.5 detector (the reason for that is explained in Ref. [17]). The theory, however, does not rule out the possibility that those priors might exist. And although they do not appear to exist for the case shown in the last panel of Fig. 1, they have been seen in other cases. One such example is shown in Fig. 7, which differs from the examples in Fig. 1 in the choice of the spectral dimension: $d = 9$ in Fig. 1, and $d = 144$ in Fig. 7. (Note that there is no extra computation time or memory expense in using the larger spectral dimension because all of the detectors can be expressed in two-dimensional matched-filter-residual (MFR) coordinates [20].)

[‡]<https://docs.scipy.org/doc/scipy/reference/optimize.html>

REFERENCES

1. A. Schaum and A. Stocker, "Spectrally selective target detection," *Proc. ISSSR (International Symposium on Spectral Sensing Research)*, p. 23, 1997.
2. D. Manolakis, "Taxonomy of detection algorithms for hyperspectral imaging applications," *Optical Engineering* **44**, p. 066403, 2005.
3. S. Matteoli, M. Diani, and J. Theiler, "An overview of background modeling for detection of targets and anomalies in hyperspectral remotely sensed imagery," *J. Selected Topics in Applied Earth Observations and Remote Sensing (JSTARS)* **7**, pp. 2317–2336, 2014.
4. D. G. Manolakis, R. B. Lockwood, and T. W. Cooley, *Hyperspectral Imaging Remote Sensing: Physics, Sensors, and Algorithms*, Cambridge University Press, Cambridge, 2016.
5. J. Theiler, B. Zimmer, and A. Ziemann, "Closed-form detector for solid sub-pixel targets in multivariate t -distributed background clutter," *Proc. IEEE International Geoscience and Remote Sensing Symposium (IGARSS)*, pp. 2773–2776, 2018.
6. A. Ziemann, M. Kucer, and J. Theiler, "A machine learning approach to hyperspectral detection of solid targets," *Proc. SPIE* **10644**, p. 1064404, 2018.
7. O. Besson and F. Vincent, "Sub-pixel detection in hyperspectral imaging with elliptically contoured t -distributed background," *arXiv 2003.11780 [eess.SP]*, 26 March 2020.
8. F. Vincent and O. Besson, "One-step generalized likelihood ratio test for subpixel target detection in hyperspectral imaging," *IEEE Trans. Geoscience and Remote Sensing* **58**, pp. 4479–4489, 2020.
9. J. Theiler, "Generalized likelihood ratio test detector for a modified replacement model target in a multivariate t -distributed background," *arXiv:2007.12662 [eess.SP]*, 24 July 2020.
10. S. M. Kay, *Fundamentals of Statistical Signal Processing: Detection Theory*, vol. II, Prentice Hall, New Jersey, 1998.
11. E. L. Lehmann and J. P. Romano, *Testing Statistical Hypotheses*, Springer, New York, 2005.
12. J. Chen, "Penalized likelihood-ratio test for finite mixture models with multinomial observations," *Canadian Journal of Statistics* **26**, pp. 583–599, 1998.
13. A. Schaum, "Continuum fusion: a theory of inference, with applications to hyperspectral detection," *Optics Express* **18**, pp. 8171–8181, 2010.
14. J. Theiler, "Confusion and clairvoyance: some remarks on the composite hypothesis testing problem," *Proc. SPIE* **8390**, p. 839003, 2012.
15. A. Schaum, "Clairvoyant fusion: a new methodology for designing robust detection algorithms," *Proc. SPIE* **10004**, p. 100040C, 2016.
16. J. Theiler, "Veritas: an admissible detector for targets of unknown strength," *Proc. SPIE* **11727**, p. 117270B, 2021.
17. J. Theiler, "Bayesian vs generalized likelihood ratio detection of solid sub-pixel targets," *Proc. International Geophysics and Remote Sensing Symposium (IGARSS)*, 2023.
18. J. Theiler, "Homeopathic priors?," *arXiv:2212.02725*, 2022.
19. J. Theiler, "Matched-pair machine learning," *Technometrics* **55**, pp. 536–547, 2013.
20. B. R. Foy, J. Theiler, and A. M. Fraser, "Decision boundaries in two dimensions for target detection in hyperspectral imagery," *Optics Express* **17**, pp. 17391–17411, 2009.